SUPPLEMENTARY INFORMATION

Conservatism and novelty in the genetic architecture of adaptation in *Heliconius* butterflies

Bárbara Huber, Annabel Whibley, Yann Le Poul, Nicolas Navarro, Arnaud Martin, Simon Baxter, Abhijeet Shah, Benoît Gilles, Thierry Wirth, W. Owen McMillan, Mathieu Joron.

SUPPLEMENTARY METHODS

GENOTYPING METHODS

Markers were first amplified in brood parents, then in the progeny when allelic variation was found. Where possible, allelic variation was scored using amplicon length variation in 3% agarose gels stained with SYBR®Safe. In the absence of clear size variation, but where Sanger sequencing revealed an appropriate restriction enzyme site difference within the amplicon, size differences in restriction digestion profiles were used to infer genotype. In two cases, competitive allele-specific PCR KASP™ assays (LGC Genomics, UK) were used, following the manufacturer's protocol, with fluorescence measured in a CFX96 Bio-Rad Real-Time PCR machine. In other cases, direct Sanger sequencing of PCR products was used. A list of the used markers and more details about the genotyping methods are given in Table S3.

PCR CONDITIONS

Standard PCR master mixes and thermal cycling conditions were used. PCR mixes contained 10–50 ng of genomic DNA, 1X reaction buffer with 2 mM $MgCl_2$, 0.1 mM each dNTP, 50 pmol of each primer and 0.25 U DreamTaq polymerase (Fermentas). Thermal cycling conditions were 94°C for 1 min, 35 cycles of 94°C for 15 sec, 55°C annealing for 30 sec, 72°C for 60 sec, and a final extension at 72°C for minutes.

MULTIVARIATE QUANTITAVE TRAIT LOCUS (QTL) ANALYSIS

Mapping colour pattern loci. Taking distinct nested subsets of Principal Components (PCs) derived from Color Pattern Modelling (CPM) may change genome association profiles slightly. Therefore, to detect the most robust QTL peaks we explored genome association profiles using different subsets of axes by incrementing the number of added PCs. The subset of axes containing all PCs explaining more than 2% of variance in the PCA was chosen. Additionally, we explored subsets that encompassed an increasing number of components accounting for down to 1% of explained variance, which revealed additional suggestive QTLs, especially on linkage groups known to harbour wing patterning loci or QTLs in other species.

The effect of an additive colour QTL was estimated using Haley-Knott regression (Haley and Knott, 1992; Knott and Haley, 2000) by fitting the multivariate linear model $\mathbf{y}_i|\mathbf{M}_i \sim N_q\left(\boldsymbol{\mu} + \sum_c x_{ic}\boldsymbol{\beta}_c + \sum_j p_{ij}\boldsymbol{\beta}_j, \mathbf{S}\right)$ where x_{ic} is the value of the covariate c and $p_{ij} = \Pr\left(g_i = j|\mathbf{M}_i\right)$ is the probability of the QTL genotypes given the flanking markers for individual i and the $\boldsymbol{\beta}$ are the q-dimensional effect of the covariate c or of the genotype j. These probabilities were computed using *R/qtl* (Broman *et al.*, 2003) at each centimorgan along the 20 autosomal chromosomes considering a genotyping error rate of 10^{-3} and the Kosambi map function (Broman *et al.*, 2002). Presence of the QTL was evaluated using the Pillai trace criterion (Pillai, 1967). The probabilities associated with its approximated F statistics were transformed to their negative $\log_{10}$ to make results comparable with LOD scores (Leamy *et al.*, 2008). All computations for colour pattern QTL mapping were conducted in the *R/shapeQTL* package written by Nicolas Navarro and available under request.

Genome-wide significance threshold. Genome-wide significance for the presence of a QTL was evaluated using a permutation approach (Churchill and Doerge, 1994). The trait together with its covariate (sex) was reshuffled among individuals whereas the original genotype probabilities were kept constant. The genome scan was repeated on these data and the maximal score (LOD) was recorded for each of 1000 iterations. We took the 90th quantile of that distribution as the 10% genome-wide threshold to detect QTLs, but defined QTLs with LOD ≥ 3 as being suggestive.

Multiple QTL modeling. We adopted an approach for model search including or dropping QTLs without any prior on the number of QTLs per chromosome following the approach developed for univariate traits by Broman and collaborators (Broman and Speed, 2002; Manichaikul *et al.*, 2009; Broman and Sen, 2009). Searches were restricted to additive QTLs only. Model choice was based on penalized scores using the –log10 of the *P*-value minus the model complexity times the 5% genome-wide threshold.

Interval estimates of QTL locations. To determine the credible intervals around each significant QTL peak, we used the *bayesint* function of *R/qtl* with a coverage probability of 0.95. Coverage of these intervals was proven stable and consistent across a variety of situations (Manichaikul *et al.*, 2006). Intervals were computed from the chromosome profile of the QTL conditional on all other refined QTL positions.

QTL effects, effect sizes and visualization. QTL effects were estimated conditional on the covariate (sex) and other QTLs included in the final model using multivariate regression of phenotypes on the backcross parameterization of QTL genotype probabilities. The effect of each colour pattern QTL was visualized within Color Patterning Modeling (CPM).

Test for epistatic interactions. Epistatic interactions between the uncovered QTLs were tested for by implementing a multivariate linear model with additive pairwise interaction between the QTLs.

SUPPLEMENTARY TABLES

Table S1. Summary table of major and minor effect wing colour pattern loci mapped in the genus *Heliconius*

Linkage group	Colour locus[A]	Causal gene	Phenotypic effect[B]	Species[C]	Loci interacting epistatically with major effect loci	References
1	***K, Khw***		White/yellow switch of background elements	*H. melpomene/cydno*		Jiggins *et al*., 2005; Joron *et al*., 2006; Kapan, 1998; Kronforst *et al*., 2006b; Linares, 1997; Naisbit *et al.,*2003
	HhK		White/yellow switch of FW band	*H. hecale*		This study
			Quantitative FW pattern variation	*H. numata*		Jones *et al.*, 2011
2			Red FW band shape	*H. melpomene*		Baxter *et al*., 2008a
	*		Red patterns on both FW and HW	*H. erato*		Nadeau *et al*., 2014
7			Red FW band shape	*H. melpomene*		Baxter *et al*., 2008a
10	***Sd, HeSd, St, Ly, c-spot***	*WntA*	Length and shape of yellow FW patch	*H. erato/himera*	*HeD, Cr*	Kapan *et al.,* 2006; Kronforst *et al*., 2006a; Mallet, 1989; Martin *et al*., 2012; Nadeau *et al*. 2014; Papa *et al*., 2013; Sheppard *et al*., 1985
	Ac, HmAc	*WntA*	Shape of FW medial band and discal "hourglass" pattern	*H. melpomene*		Jiggins *et al.*, 2005; Kronforst *et al.*, 2006a; Martin *et al*., 2012; Nijhout *et al.*, 1990; Sheppard *et al.,* 1985
	Ac, Ps	*WntA*	Discal "hourglass" pattern of FW and width of HW bar	*H. cydno/pachinus*		Gallant *et al*., 2014; Gilbert, 2003; Kronforst *et al*., 2006a; Martin *et al.*, 2012; Nijhout *et al.*, 1990
	HhAc	*WntA*	Melanisation close to FW discal cell	*H. hecale*	Hspot	This study
	HiAc	*WntA*	Melanisation close to FW discal cell	*H. ismenius*		This study
	*****		Yellow HW band	*H. erato*		Nadeau *et al.,* 2014
			Quantitative FW and HW pattern variation	*H. numata*		Jones *et al*., 2011
			Red FW band shape	*H. melpomene*		Baxter *et al.*, 2008a

Table S1. *Continued*

Linkage group	Colour locus[A]	Causal gene	Phenotypic effect[B]	Species[C]	Loci interacting epistatically with major effect loci	References
13	*Ro*		Rounding of the distal edge of the upper FW band	*H. erato*		Nadeau *et al*., 2014
			Red FW band shape	*H. melpomene*		Baxter *et al*., 2008a
15	***Supergene P***		Whole FW and HW variation	*H. numata*		Jones *et al.*, 2011; Joron *et al.*, 2006
	Cr		HW yellow bar	*H. erato/himera*	*HeD, Sd*, non mapped modifiers	Counterman *et al.*, 2010; Kronforst *et al*., 2006a; Jiggins and McMillan, 1997; Joron *et al.,* 2006; Mallet, 1989; Papa *et al.*, 2008; Sheppard *et al.*, 1985; Tobler *et al.,* 2004
			White HW margin	*H. erato/himera*		
			Medial yellow FW band	*H. erato/himera*		
	Yb, HmYb, Cs		Yellow HW bar	*H. melpomene/cydno*	*Br*	Emsley, 1964; Ferguson *et al*., 2010; Kronforst *et al.,* 2006a; Jiggins *et al.*, 2005; Joron *et al*., 2006; Linares, 1997; Mallet, 1989; Nadeau *et al.*, 2014; Naisbit *et al.*, 2003; Nijhout *et al.,* 1990; Sheppard *et al.*, 1985
			Pink/orange switch on ventral side of FW band	*H. melpomene*		Baxter *et al*., 2008a
	Sb		White or yellow HW margin	*H. melpomene/cydno*	Non mapped locus *L*	Emsley, 1964; Ferguson *et al*., 2010; Jiggins *et al.*, 2005; Joron *et al.,* 2006; Linares, 1996; Linares, 1997; Naisbit *et al*., 2003
	Hspot		Marginal spots on HW	*H. hecale*	*HhAc*	This study
	N		Yellow colour in the medial FW band	*H. melpomene*	*HmB, HmD*	Mallet, 1989; Nadeau *et al.*, 2014; Sheppard *et al.*, 1985
	HhN		Subapical row of spots on FW	*H. hecale*		This study
	HiN		Shape of distal edge of FW band	*H. ismenius*		This study
	Fspot		Apical row of spots on FW	*H. hecale*		This study

Table S1. *Continued*

Linkage group	Colour locus[A]	Causal gene	Phenotypic effect[B]	Species[C]	Loci interacting epistatically with major effect loci	References
17	*		Yellow HW bar	*H. erato*		Nadeau *et al*., 2014
18	***HeD, D, DRY***	*optix*	Red FW ‘‘dennis’’	*H. erato/himera*	*Sd, Cr*, non mapped modifiers	Baxter *et al*., 2008b; Counterman *et al*., 2010; Jiggins and McMillan, 1997; Kapan, 2006; Mallet, 1989; Martin *et al.,* 2014; Nadeau *et al.*, 2014; Papa *et al.*, 2008; Reed *et al*., 2011; Sheppard *et al.*, 1985; Tobler *et al.*, 2005
		optix	Red HW rays	*H. erato/himera*		
		optix	Red/yellow FW	*H. erato/himera*		
	HmD, D	*optix*	Red HW "rays" and proximal "dennis" patches on both wings	*H. melpomene*	*N*	Baxter *et al.*, 2008b; Mallet, 1989; Nadeau *et al*., 2014; Reed *et al.*, 2011; Sheppard *et al.,* 1985; Turner and Crane, 1962
	HmB, B	*optix*	Red medial FW band	*H. melpomene*	*N*	Baxter *et al.*, 2008b; Mallet, 1989; Martin *et al*., 2014; Reed *et al.*, 2011; Sheppard, 1985; Turner and Crane, 1962; Turner, 1972
	Br, “forceps” shutter	*optix*	Brown oval pattern on the ventral side of the HW	*H. cydno/pachinus*	*Yb*	Chamberlain *et al.*, 2011; Gilbert, 2003; Naisbit *et al*., 2003; Reed *et al.*, 2011
	HhBr		Shape of marginal black band on HW	*H. hecale*		This study
	HiBr		Shape of marginal black band on HW	*H. ismenius*		This study
	G, basal red	*optix*	Basal HW red spots and basal FW small bar	*H. melpomene/cydno/ pachinus*		Chamberlain *et al.*, 2011; Gilbert, 2003; Kronforst *et al.*, 2006a; Linares, 1996; Martin *et al*., 2014; Naisbit *et al.*, 2003
	Wh (possibly)		White/yellow switch of FW band	*H. erato/himera*		Papa *et al.*, 2013; Sheppard *et al.*, 1985
	Cm		HW and proximal FW melanisation	*H. hecale*		This study
			Middle FW band size and shape	*H. erato/himera*		Papa *et al.,* 2013
			Quantitative FW pattern variation	*H. numata*		Jones *et al*., 2011
19			Quantitative FW pattern variation	*H. numata*		Jones *et al*., 2011

Table S1. *Continued*

Linkage group	Colour locus[A]	Causal gene	Phenotypic effect[B]	Species[C]	Loci interacting epistatically with major effect loci	References
Sex Z chromosome			Red FW band shape	*H. melpomene*		Baxter *et al*., 2008a
			FW band shape	*H. erato*		Mallet, 1989
			"Whiteness" (or "yellowness") of FW band	*H. erato/himera*		Papa *et al*., 2013
			Quantitative FW and HW pattern variation	*H. numata*		Jones *et al.*, 2011

[A]Some loci have alternative names separated by commas. The name of major effect loci is written in bold script. QTLs that were named in this study are written in non-italic script.

[B]Abbreviations FW and HW correspond to forewing(s) and hindwing(s), respectively.

[C]Species in which a given locus was described. Slashes separate species that were intercrossed to infer gene homology.

*Low confidence genotype-to-phenotype association.

Table S2. Sampling localities for the specimens of *Heliconius hecale* and *H. ismenius* used in the crosses

Species	Race	Country	Locality	GPS coordinates
Heliconius hecale	*melicerta*	Panamá	Gamboa, Colón	N9°7.257, W79°43.591
	zuleika	Panamá	Miramar, Bocas del Toro	N8°59.369, W82°14.597
	clearei	Venezuela	Tumeremo, Bolívar	N6°50.185, W61°35.554
Heliconius ismenius	*boulleti*	Panamá	Yaviza, Darién	N8°16.783, W77°48.589
	telchinia	Panamá	Miramar, Bocas del Toro	N8°59.369, W82°14.597

Table S3. List of markers used to fine-map colour loci in *H. hecale* and *H. ismenius*

Marker name	Marker type (*Annotation on H. melpomene genome*)	Scaffold (starting position on *H. melpomene* genome)	Primer sequence	Genotyping method (*enzyme*)	Genotyped brood(s)
Around *HhK*					
KASP_Wg	SNP	HE671174 (588001)	NA[7]	KASP™ assays[6]	Br112, Br117
Wingless_F1	EPIC[1] (*HMEL022601*)	HE671174 (1166344)	ATGCTAGTATCGTTGCAGGC	Sanger sequencing	Br112
Wingless_R1		HE671174 (1167592)	CACAACAATGAAGCCGGCAG		
scf670889_geno_F3	Non-coding	HE670889 (74431)	GACATCTCTGAGTGTGAC	dCAPS[2] (*EcoRI*)	Br112
scf670889_geno_R3a		HE670889 (75124)	ACGCGAGCTTCATTCCGCGA		
KASP_Trib2	SNP	HE670375 (50059)	NA[7]	KASP™ assays[6]	Br112
EN10_F3[4]	SCNL[3] (*HMEL011986*)	HE671246 (~65983)	ACCAGCTGGACATGATGAGRA	Restriction profiles (*HindIII*)	Br112, Br117
EN10_R2[4]		HE671246 (66241)	ACGRTARGCCTTCAAAGTCARGAAT		
BAP28_F2[4]	SCNL[3] (*HMEL002583*)	HE668177 (139034)	GATCAAAAATGTATCAGTCC	Sanger sequencing	Br112
BAP28_R2[4]		HE668177 (139761)	GTTATTATCTGGAAGCTGTA		
Around *HhAc*/*HiAc*					
WntAscf_geno_F3	Non-coding	HE668478 (318250)	CTGATACATTGATGAGGA	Sanger sequencing + Amplicon length polymorphism	Br122, Br96, Br101
WntAscf_geno_R3		HE668478 (319228)	CTCGGAGCCACTCCTGAC		
WntAscf_geno_F6	Non-coding intergenic (*HMEL002905-HMEL002906*)	HE668478 (402431)	GTCCTAGCAACTAAGTTC	Restriction profiles (*TaqI*)	Br122
WntAscf_geno_R6a		HE668478 (403235)	GACAKGCTTGGTCATCCA		
WntAscf_geno_F6	Non-coding intergenic (*HMEL002905-HMEL002906*)	HE668478 (402431)	GTCCTAGCAACTAAGTTC	Sanger sequencing	Br96, Br101
WntAscf_geno_R6b		HE668478 (403501)	ACTTCTTCGCAGRGGTACA		
WntA_F[5]	EPIC[1] (*HMEL018100*)	HE668478 (481158)	CAGGCGGTACGTGGTCGT	Sanger sequencing	Br122
WntA_R[5]		HE668478 (482177)	CGGCTCACAATAGTCCGGG		
Chitsynth3_F[5]	EPIC[1] (*HMEL018102*)	HE668478 (497654)	CCTTCGACGATGGTGTAAACGTGCAAA	Sanger sequencing	Br96, Br101
Chitsynth3_R[5]		HE668478 (497048)	AGGCACTGGGGCAAGGTGGC		
scf669520_geno_F2	EPIC[1] (*HMEL004236*)	HE669520 (87479)	AGTCCTSGGTCCAGCGGA	Amplicon length polymorphism	Br122
scf669520_geno_R2		HE669520 (88848)	GGTTCTTCRACCACTTCA		

Table S3. *Continued*

Marker name	Kind of marker (*alternative locus name*)	Scaffold (starting position on *H.melpomene* reference)	Primer sequence	Genotyping method (*enzyme*)	Genotyped brood(s)
Around *HhN*/*HiN*					
Fizzyscf_geno_F5b Fizzyscf_geno_R5	EPIC[1] (*HMEL000008*)	HE667780 (499593) HE667780 (500190)	GCTGCACTGCCGCCAGCTGA GCTCRTCCGCTCGCATTA	Sanger sequencing	Br122
Gene25_ex7_F Gene25_ex7_R	EPIC[1] (*HMEL000025*). Partially non-coding	HE667780 (670937) HE667780 (670240)	TCTTCCAATTTAARCTAAYGTCG TTGCGATGTCCGCACCTGACG	Sanger sequencing	Br96, Br101
Hn25_fizz_F1 Gene25_ex1_R	EPIC[1] (*HMEL000025*)	HE667780 (680510) HE667780 (679516)	CGCAACGTTATCGCCTAGAT GAAGCTGAAAGCGAAAGMAC	Sanger sequencing + Restriction profiles (XhoI)	Br96, Br101, Br112
Fizzyscf_geno_F4 Fizzyscf_geno_R4	EPIC[1] (*HMEL002028*). Partially non-coding	HE667780 (841439) HE667780 (842349)	TGGTGGGAATACGCAAGGA TGGACTGTCGGCTTTAAGC	Sanger sequencing	Br96, Br101
Fizzyscf_geno_F8 Fizzyscf_geno_R8	EPIC[1] (*HMEL000041*)	HE667780 (1030768) HE667780 (1031999)	ACCTCAGAGTGTCCGAGCTC GATGGTCCAATCAGACTGGC	Sanger sequencing	Br96, Br101
Around *HhBr*/*HiBr*					
Optixscf_geno_F5 Optixscf_geno_R5	Non-coding intergenic + partial exons (*HMEL001009-HMEL001022*)	HE670865 (251935) HE670865 (253169)	CATCCCGATCGCTAAGGCAC CAACTTACASCATCAACTGAC	Sanger sequencing	Br96, Br101
Optixscf_geno_F6 Optixscf_geno_R6	EPIC[1] (*HMEL001018*)	HE670865 (285696) HE670865 (287142)	ATACAGGACTGGGCTCTGA CCCAGCTCATTGGAAAGC	Sanger sequencing	Br122, Br120
Optixscf_geno_F14 Optixscf_geno_R14	EPIC[1] (*HMEL001014*)	HE670865 (308062) HE670865 (308886)	CATCTTTCAGGGAAGTATGG GCACATTGCCACGGCTCG	Restriction profiles (*TaqI*)	Br96, Br101
HmB453k_geno_F HmB453k_geno_R	Non-coding	HE670865 (375602) HE670865 (376487)	AGGTTCYCSAGACGGTATCCTCA CCGTTGGGTATCCGTAAAGCC	Amplicon length polymorphism	Br122
Optixscf_geno_F1 Optixscf_geno_R1	Non-coding	HE670865 (380464) HE670865 (381718)	GAGACATRTTARTTTTCTCTGCC CACCACTTTGAAAGGAATCGTA	Restriction profiles (*SpHI-HF* + *TaqI*)	Br96, Br101, Br112
Optixscf_geno_F2 Optixscf_geno_R2	Non-coding	HE670865 (388302) HE670865 (389396)	GTTCTGACTTCTGAGATCATCAT AGGCATAGACAGTTGAGCGGAGA	Amplicon length polymorphism	Br122
Optixscf_geno_F10 Optixscf_geno_R10	EPIC[1] (*HMEL001038*)	HE670865 (498086) HE670865 (499708)	ACGCCCATTCAGGTAGCCTC GTGGTATTGAACGATGGTC	Sanger sequencing	Br96, Br101

[1]Exon-primed intron-crossing

[2]Derived Cleaved Amplified Polymorphic Sequences

[3]Single-copy nuclear loci

[4]Marcus Kronforst, *personal communication*

[5]Martin *et al.*, 2012

[6]Kompetitive Allele Specific PCR (LGC Genomics)

[7]Not applicable

Table S4. Allelic segregation of colour pattern loci in the mapping families of *H. hecale* and *H. ismenius*

***Heliconius hecale melicerta* x *H. hecale clearei* crosses**										
FAMILY	**COLOUR LOCUS**	**PATERNAL GENOTYPE**	**MATERNAL GENOTYPE**	**NUMBER OF PROGENY**				**EXPECTED MENDELIAN RATIO**	**χ^2**	***P*-VALUE**
				HhK_cHhK_m		***HhK_mHhK_m***	**Not scored**			
Br112	***HhK***	*HhK_cHhK_m*	*HhK_mHhK_m*	84		98	0	1:1	1.0769	0.2994
Br117		*HhK_cHhK_m*	*HhK_mHhK_m*	49		58	0	1:1	0.7570	0.3843
Br112+Br117		NA	NA	133		156	0	1:1	1.8304	0.1761
***Heliconius hecale melicerta* x *H. hecale zuleika* crosses**										
FAMILY	**COLOUR LOCUS**	**PATERNAL GENOTYPE**	**MATERNAL GENOTYPE**	**NUMBER OF PROGENY**				**EXPECTED MENDELIAN RATIO**	**χ^2**	***P*-VALUE**
				$HhAc_zHhAc_m$		***$HhAc_mHhAc_m$***	**Not scored**			
Br122	***HhAc***	*$HhAc_zHhAc_m$*	*$HhAc_mHhAc_m$*	46		50	1	1:1	0.1667	0.6831
Br120		*$HhAc_zHhAc_m$*	*$HhAc_mHhAc_m$*	7		12	3	1:1	1.3158	0.2513
Br120+Br122		NA	NA	53		62	4	1:1	0.7043	0.4013
				HhN_zHhN_z	***HhN_zHhN_m***	***HhN_mHhN_m***	**Not scored**			
Br122	***HhN***	*HhN_zHhN_m*	*HhN_zHhN_m*	26	32	27	13	1 :2 :1	3.6558	0.1607
Br120		*HhN_zHhN_m*	*HhN_mHhN_m*	NA	11	7	4	1:1	0.8889	0.3458
Br120+Br122		NA	NA	NA	NA	NA	NA	NA	NA	NA
				$HhBr_zHhBr_m$		***$HhBr_mHhBr_m$***	**Not scored**			
Br122	***HhBr***	*$HhBr_zHhBr_m$*	*$HhBr_mHhBr_m$*	49		44	5	1:1	0.2688	0.6041
Br120		*$HhBr_zHhBr_m$*	*$HhBr_mHhBr_m$*	8		11	3	1:1	0.4737	0.4913
Br120+Br122		NA	NA	57		55	8	1:1	0.0357	0.8501

Table S4. *Continued*

***Heliconius ismenius boulleti* x *H. ismenius telchinia* crosses**									
FAMILY	**COLOUR LOCUS**	**PATERNAL GENOTYPE**	**MATERNAL GENOTYPE**	**NUMBER OF PROGENY**			**EXPECTED MENDELIAN RATIO**	**χ^2**	***P*-VALUE**
				$HiAc_tHiAc_b$	$HiAc_bHiAc_b$	**Not scored**			
Br96	***HiAc***	$HiAc_tHiAc_b$	$HiAc_bHiAc_b$	23	13	0	1:1	2.7778	0.0956
Br101		$HiAc_tHiAc_b$	$HiAc_bHiAc_b$	8	10	0	1:1	0.2222	0.6374
Br196+Br101		NA	NA	31	23	0	1:1	1.1852	0.2763
				HiN_tHiN_b	HiN_bHiN_b	**Not scored**			
Br96	***HiN***	HiN_tHiN_b	HiN_bHiN_b	15	21	0	1:1	1	0.3173
Br101		HiN_tHiN_b	HiN_bHiN_b	8	10	0	1:1	0.2222	0.6374
Br196+Br101		NA	NA	23	31	0	1:1	1.1852	0.2763
				$HiBr_tHiBr_b$	$HiBr_bHiBr_b$	**Not scored**			
Br96	***HiBr***	$HiBr_tHiBr_b$	$HiBr_bHiBr_b$	16	20	0	1:1	0.4444	0.505
Br101		$HiBr_tHiBr_b$	$HiBr_bHiBr_b$	11	7	0	1:1	0.8889	0.3458
Br196+Br101		NA	NA	27	27	0	1:1	0	1

Table S5. Summary of RAD library sequencing and mapping statistics.

	Library 1 (*melicerta* x *zuleika*) N=64		Library 2 (*melicerta* x *clearei*) N=64		Library 3 (*boulleti* x *telchinia* mainly) N=64		All libraries combined N=192	
Filtering steps	**Number of reads**	**Percentage (%)[1]**	**Number of reads**	**Percentage (%)[1]**	**Number of reads**	**Percentage (%)[1]**	**Number of reads**	**Percentage (%)[1]**
Sequenced reads	247,783,430		162,166,578		343,911,015		753,861,023	
Retained reads	188,974,386	76.27	137,315,022	84.68	290,156,532	84.37	616,445,940	**81.77**
Mapped reads	177,609,643	93.99	129,572,241	94.36	272,334,861	93.86	579,516,745	**94.01**
Reads after deduplication	23,454,960	13.21	16,954,588	13.09	26,418,741	9.70	66,828,289	**11.53**
		9.47[2]		10.46[2]		7.68[2]		**8.86[2]**

[1]Percentage is expressed relative to the number of reads in the previous filtering step

[2]Percentage of reads after deduplication relative to the total number of sequenced reads

Table S6. Number of per-individual 100-bp Illumina reads (sequenced and filtered through the first quality filtering steps) in Library 1 (Brood 122: *H. hecale melicerta* x *H. h. zuleika)*

Barcode	Sample	Sequenced reads	Retained reads	Mapped reads	Reads after deduplication
CGATA	**MJ11-2718**[1]	**25 732 118**	**18 438 392**	**16 778 275**	**1 045 850**
ACACG	MJ11-2688	9 948 346	7 205 156	6 791 939	949 641
CCAAC	MJ11-2779	9 939 526	7 779 076	7 337 787	912 266
ATATC	MJ11-2731	10 319 068	7 483 572	7 059 846	907 840
AGGAC	MJ11-2730	9 181 841	7 292 064	6 918 616	892 152
ATGCT	MJ11-2776	9 207 657	7 267 068	6 886 915	877 760
CGGCG	**MJ11-2463**[2]	**8 396 067**	**6 994 052**	**6 626 957**	**854 830**
AGAGT	MJ11-2729	8 855 104	6 591 020	6 252 333	847 735
CCGGT	MJ11-2780	8 858 882	7 125 696	6 548 152	844 874
CAGTC	MJ11-2778	8 446 873	6 659 330	6 284 163	838 981
CAACT	MJ11-2777	8 374 724	6 177 230	5 830 719	806 271
TTGGC	MJ11-2642	6 671 879	5 386 058	5 026 425	739 315
AAAAA	MJ11-2685	6 210 214	4 324 324	4 105 322	667 760
GCATT	MJ11-2612	5 442 139	4 441 378	4 223 045	579 166
GGAAG	MJ11-2614	5 164 532	4 049 114	3 848 970	554 353
AAGGG	MJ11-2686	5 479 533	2 903 670	2 743 489	509 770
GCGCC	MJ11-2613	4 379 898	3 631 954	3 449 297	499 812
GGGGA	MJ11-2616	4 541 978	3 617 850	3 440 234	499 135
TAGCA	MJ11-2630	4 546 801	3 690 104	3 502 306	490 533
TGGTT	MJ11-2640	4 284 587	3 425 896	3 259 201	475 009
GAAGC	MJ11-2591	4 057 737	3 302 644	3 137 934	465 573
ACGTA	MJ11-2728	3 997 431	2 602 282	2 435 934	451 995
TAATG	MJ11-2627	4 060 992	3 208 364	3 053 018	443 538
GTGTG	MJ11-2626	3 929 706	3 096 300	2 943 795	431 993
CTAGG	MJ11-2580	3 577 563	2 814 156	2 672 368	403 496
GAGAT	MJ11-2596	3 298 722	2 410 394	2 223 612	338 276
CATGA	MJ11-2813	4 861 128	3 930 732	3 617 383	337 509
TCTCT	MJ11-2963	4 956 151	3 547 176	3 260 669	321 423
GTCAC	MJ11-2786	1 928 458	1 584 916	1 495 332	316 396
GGTTC	MJ11-2787	1 662 645	1 375 690	1 298 944	283 395
TATAC	MJ11-2965	2 193 856	1 730 656	1 639 341	275 326
TCAGA	MJ11-2637	2 322 884	1 788 856	1 698 940	272 777
TGCAA	MJ11-2848	3 302 057	2 779 298	2 618 276	267 625
TTTTA	MJ11-2845	3 255 758	2 436 620	2 304 275	254 513
TTAAT	MJ11-2641	2 067 017	1 602 960	1 516 407	247 341
TGTGG	MJ11-2847	3 202 932	2 453 990	2 304 730	244 115
GGCCT	MJ11-2788	1 343 268	1 065 984	1 009 162	234 640
TACGT	MJ11-2966	1 901 846	1 532 234	1 451 874	232 105
TCCTC	MJ11-2964	1 598 237	1 272 922	1 205 446	210 738
CACAG	MJ11-2844	2 758 648	1 958 736	1 844 666	207 073
CCCCA	MJ11-2812	2 199 867	1 804 264	1 702 524	202 929
TTCCG	MJ11-2846	2 298 902	1 863 760	1 756 883	197 950

Table S6. *Continued*

Barcode	Sample	Sequenced reads	Retained reads	Mapped reads	Reads after deduplication
TGACC	MJ11-2639	1 479 142	1 158 840	1 101 095	192 258
CTGAA	MJ11-2581	1 484 154	1 143 548	1 086 926	183 045
GTACA	MJ11-2625	1 470 511	1 078 542	1 023 942	174 039
CGCGC	MJ11-2810	1 402 412	1 212 288	1 132 074	140 201
CGTAT	MJ11-2809	1 925 999	1 229 322	1 165 702	138 446
CTCTT	MJ11-2808	1 469 152	1 129 968	1 072 183	135 665
TCGAG	MJ11-2638	1 066 706	692 680	658 963	114 911
GTTGT	MJ11-2785	604 765	449 850	427 501	108 821
GACTA	MJ11-2804	1 044 231	892 068	848 964	107 587
ATCGA	MJ11-2784	564 604	432 496	408 847	105 636
CTTCC	MJ11-2807	1 015 487	785 930	744 019	94 790
GATCG	MJ11-2791	1 122 903	837 066	725 156	92 291
AGCTG	MJ11-2806	873 478	712 370	670 957	88 462
GCTAA	MJ11-2789	854 270	708 964	671 480	84 591
CCTTG	MJ11-2811	922 259	668 524	633 733	82 567
AGTCA	MJ11-2805	703 939	563 242	533 604	70 742
GCCGG	MJ11-2790	548 449	461 576	436 666	59 917
ATTAG	MJ11-2782	350 203	165 148	156 696	44 637
ACTGC	MJ11-2657	20 076	1 760	1 655	798
AATTT	MJ11-2653	49 739	1 630	1 489	683
AACCC	MJ11-2651	9 263	1 276	1 198	549
ACCAT	MJ11-2656	44 116	1 360	1 289	544
	Total	**247 783 430**	**188 974 386**	**177 609 643**	**23 454 960**

[1]Mother of brood 122

[2]Father of brood 122

Table S7. Number of per-individual 100-bp Illumina reads (sequenced and filtered through the first quality filtering steps) in Library 2 (Brood 112: *H. hecale melicerta* x *H. h. clearei*)

Barcode	Sample	Sequenced reads	Retained reads	Mapped reads	Reads after deduplication
CGATA	**MJ11-2706[1]**	**31 586 600**	**26 752 988**	**24 751 360**	**1 753 361**
CGGCG	**MJ11-2296[2]**	**8 892 296**	**7 738 266**	**7 313 679**	**1 085 291**
CAGTC	MJ11-2711	5 281 174	1 560 946	1 485 986	479 463
GAAGC	MJ11-2430	3 056 550	2 112 546	2 007 728	478 822
AAGGG	MJ11-2670	5 328 565	2 630 936	2 513 321	469 090
AGAGT	MJ11-2690	5 307 831	2 461 396	2 348 132	460 205
ACACG	MJ11-2672	4 686 169	2 370 502	2 269 696	451 060
GAGAT	MJ11-2432	3 054 033	2 265 006	2 159 296	440 877
TCGAG	MJ11-2543	2 905 596	2 304 474	2 192 958	439 031
TAGCA	MJ11-2522	2 867 345	2 064 096	1 967 730	438 357
GCATT	MJ11-2433	2 818 020	1 608 594	1 530 684	424 645
GCGCC	MJ11-2467	2 610 108	1 988 918	1 893 799	419 014
TAATG	MJ11-2521	2 687 770	2 198 134	2 093 376	414 354
ATATC	MJ11-2693	4 653 598	2 377 810	2 270 310	414 315
GGAAG	MJ11-2483	2 845 371	2 108 804	2 000 793	413 891
CCGGT	MJ11-2715	4 349 906	2 407 456	2 292 018	405 284
TCAGA	MJ11-2539	2 481 961	697 724	663 884	395 128
ACGTA	MJ11-2678	4 390 208	898 550	843 157	394 874
CAACT	MJ11-2708	4 215 097	984 888	936 834	393 694
CTGAA	MJ11-2428	2 517 675	1 772 692	1 681 187	393 525
AGGAC	MJ11-2691	4 221 221	4 684	4 396	392 870
GGGGA	MJ11-2486	2 466 810	4 558	4 030	391 989
ATGCT	MJ11-2695	4 271 691	3 956	3 478	391 671
CCAAC	MJ11-2714	4 335 602	3 076	2 781	383 291
GTGTG	MJ11-2492	2 444 909	3 518 438	3 237 167	370 833
AAAAA	MJ11-2648	4 053 702	4 388 290	4 182 964	369 351
TTGGC	MJ11-2593	2 102 579	4 031 774	3 846 639	343 279
GTACA	MJ11-2491	2 004 021	3 780 838	3 582 411	314 747
CTAGG	MJ11-2403	1 919 328	4 471 800	4 268 083	308 116
TGCAA	MJ11-2874	2 101 028	3 562 670	3 370 565	208 582
TTAAT	MJ11-2592	1 179 074	3 863 334	3 662 897	199 176
TCTCT	MJ11-2882	1 925 304	3 602 622	3 422 215	198 716
TGGTT	MJ11-2578	1 175 456	3 630 180	3 433 194	182 746
TATAC	MJ11-2886	1 788 779	4 538 612	4 304 519	181 636
TCCTC	MJ11-2883	1 668 337	3 661 136	3 462 336	172 084
TTTTA	MJ11-2840	1 575 227	3 774 034	3 508 621	161 672
TGTGG	MJ11-2872	1 528 011	106 116	100 190	155 147
TACGT	MJ11-2889	1 482 460	222 490	206 870	152 859
TGACC	MJ11-2577	901 106	98 452	93 130	149 028
CCCCA	MJ11-2830	1 231 483	850 112	802 002	135 213
CATGA	MJ11-2835	1 213 001	742 494	709 037	126 761
TTCCG	MJ11-2871	1 085 307	625 206	597 542	113 251

Table S7. *Continued*

Barcode	Sample	Sequenced reads	Retained reads	Mapped reads	Reads after deduplication
GTCAC	MJ11-2753	968 012	625 700	597 286	108 186
GGTTC	MJ11-2754	849 310	188 108	142 238	95 484
GGCCT	MJ11-2755	729 743	277 804	264 490	80 997
GACTA	MJ11-2769	724 078	638 648	610 420	79 232
GCTAA	MJ11-2759	708 833	277 024	262 923	78 435
CGTAT	MJ11-2799	748 972	496 068	472 509	77 493
CGCGC	MJ11-2815	571 647	369 196	352 124	65 859
AGCTG	MJ11-2793	576 094	430 126	410 663	64 824
CTCTT	MJ11-2797	514 797	593 006	565 555	56 653
CTTCC	MJ11-2795	431 437	500 100	476 158	47 334
CCTTG	MJ11-2816	377 567	315 946	300 598	40 945
GATCG	MJ11-2763	328 597	1 057 588	1 008 614	37 489
AGTCA	MJ11-2770	323 388	1 060 754	978 067	37 018
CACAG	MJ11-2839	282 425	238 696	222 314	31 191
ATCGA	MJ11-2748	259 617	1 358 780	1 296 008	29 519
GCCGG	MJ11-2762	216 249	937 192	890 200	25 964
ATTAG	MJ11-2747	134 276	1 333 234	1 237 185	14 746
GTTGT	MJ11-2750	132 182	1 856 788	1 768 236	13 690
AATTT	MJ11-2609	29 376	1 661 118	1 587 855	649
AACCC	MJ11-2608	8 429	1 458 554	1 391 294	644
ACCAT	MJ11-2633	28 437	1 562 614	1 493 977	536
ACTGC	MJ11-2636	12 803	1 288 380	1 222 532	399
Total		**162 166 578**	**137 315 022**	**129 572 241**	**16 954 588**

[1]Mother of brood 112
[2]Father of brood 112

Table S8. Number of per-individual 100-bp Illumina reads (sequenced and filtered through the first quality filtering steps) in Library 3 (Broods 96 and 101 mainly: *H. ismenius boulleti* x *H. h. telchinia*)

Barcode	Sample	Sequenced reads	Retained reads	Mapped reads	Reads after deduplication
CTAGG	**MJ11-2264[1]**	**38 739 993**	**32 662 854**	**30 342 291**	**1 892 527**
CGATA	**MJ11-2363[2]**	**35 389 452**	**30 194 930**	**28 576 405**	**1 805 661**
CGGCG	**MJ11-2406[3]**	**20 585 884**	**17 325 512**	**15 399 581**	**1 383 246**
CAACT	MJ11-2402	11 850 348	10 062 816	9 479 636	1 142 718
AAGGG	MJ11-2329	8 458 331	6 960 246	6 539 455	918 845
GCATT	MJ11-2301	12 787 618	10 934 104	10 339 925	816 704
AAAAA	MJ11-2328	7 597 081	6 342 870	5 984 500	812 860
TGGTT	MJ11-2318	12 740 143	10 897 012	10 283 756	799 158
GAAGC	MJ11-2290	12 163 923	10 553 168	9 936 356	745 201
ATATC	MJ11-2368	7 975 510	6 518 902	6 197 532	742 741
ACACG	MJ11-2364	5 624 189	4 709 820	4 491 874	717 336
CAGTC	MJ11-2408	5 959 139	5 034 456	4 712 162	701 873
CCAAC	MJ11-2426	5 881 182	4 974 108	4 687 226	684 329
ATGCT	MJ11-2369	5 788 804	4 842 640	4 621 616	677 135
GGGGA	MJ11-2304	9 563 462	8 086 646	7 622 086	661 028
TAGCA	MJ11-2313	8 668 218	7 495 530	6 988 366	589 846
GGAAG	MJ11-2303	8 074 931	6 585 794	6 268 711	561 974
TGACC	MJ11-2317	6 893 188	5 865 872	5 462 717	529 000
TCAGA	MJ11-2315	7 144 977	6 181 174	5 884 549	516 684
GAGAT	MJ11-2300	7 201 087	5 766 030	5 457 954	513 365
GCGCC	MJ11-2302	6 894 298	5 970 946	5 685 755	513 153
CCGGT	MJ11-2427	3 846 722	3 211 670	3 031 477	501 911
GTACA	MJ11-2305	6 605 964	5 678 316	5 281 624	499 396
CTGAA	MJ11-2314	6 084 170	5 239 820	4 933 966	462 258
TAATG	MJ11-2312	6 127 570	5 031 616	4 750 616	438 485
TCGAG	MJ11-2316	5 605 360	4 749 388	4 471 598	431 093
GTGTG	MJ11-2306	5 673 645	4 796 346	4 477 293	427 402
AGAGT	MJ11-2366	3 326 990	2 630 738	2 516 304	418 175
TGCAA	MJ11-2687*	4 703 459	4 046 032	3 857 234	352 986
ACGTA	MJ11-2365	2 490 780	2 082 294	1 977 996	349 413
TCCTC	MJ11-2652*	4 034 566	3 480 000	3 307 773	318 913
TCTCT	MJ11-2849*	4 335 342	3 622 550	3 446 747	318 703
TGTGG	MJ11-2655*	4 237 022	3 618 720	3 449 153	317 078
TTGGC	MJ11-2320	3 534 799	3 039 474	2 833 474	314 358
TTCCG	MJ11-2617*	3 788 221	3 211 864	3 006 985	284 027
TATAC	MJ11-2781*	3 682 044	3 118 546	2 975 126	278 910
AGGAC	MJ11-2367	2 103 408	1 772 862	1 663 580	268 682
TTAAT	MJ11-2319	2 855 219	2 265 572	2 149 925	253 072
TTTTA	MJ11-2998	3 256 291	2 651 558	2 504 958	225 434
GGTTC	MJ11-2379	1 218 766	1 012 952	954 444	186 409
TACGT	MJ11-2771**	2 248 345	1 858 028	1 775 254	176 892
CATGA	MJ11-2574	2 113 463	1 809 542	1 670 742	163 741

Table S8. *Continued*

Barcode	Sample	Sequenced reads	Retained reads	Mapped reads	Reads after deduplication
CCCCA	MJ11-2538	1 707 097	1 472 432	1 387 340	160 200
GTCAC	MJ11-2355	942 327	794 328	742 446	150 804
CACAG	MJ11-2575	1 716 787	1 463 884	1 374 591	141 343
GGCCT	MJ11-2380	784 393	637 040	599 575	126 435
GCTAA	MJ11-2495	768 449	641 738	600 169	123 719
AGTCA	MJ11-2531	1 414 800	1 218 734	1 149 939	115 585
GTTGT	MJ11-2999	731 729	586 036	473 402	100 733
CGTAT	MJ11-2535	1 261 035	1 020 876	961 773	100 591
CTCTT	MJ11-2534	1 255 996	1 029 298	910 773	97 738
CCTTG	MJ11-2537	1 123 829	934 320	878 531	90 555
ATCGA	MJ11-2514	594 343	465 982	434 760	81 186
CGCGC	MJ11-2536	857 887	728 766	683 611	80 286
CTTCC	MJ11-2533	983 648	822 396	775 596	80 273
GATCG	MJ11-2525	449 316	374 746	352 131	77 861
GACTA	MJ11-2530	403 094	334 220	318 600	68 845
AGCTG	MJ11-2532	573 222	452 954	425 768	48 395
GCCGG	MJ11-2496	220 997	183 268	171 040	40 981
ATTAG	MJ11-2443	136 823	93 956	88 736	19 320
ACTGC	MJ11-2327	21 869	5 498	5 004	763
AACCC	MJ11-2324	8 616	696	681	162
AATTT	MJ11-2325	54 797	574	541	125
ACCAT	MJ11-2326	46 057	1 472	1 132	121
	Total	**343 911 015**	**290 156 532**	**272 334 861**	**26 418 742**

[1]Father of broods 96 and 101

[2]Mother of brood 96

[3]Mother of brood 101

*Individuals belonging to brood 122

**Individual belonging to brood 112

Table S9. Summary of RAD library marker types and segregation patterns

Cross	Genotyped sites (variable and not)[1]	Female informative markers[2]	Male informative markers[3]	Intercross markers[4]	Total informative sites	Segregation patterns[5]				Markers in maps[6]
						Supported by 1 marker	Supported by 2 markers	Supported by >=3 markers	Total	
melicerta* x *zuleika	187,559	1,066	1,106	484	2,656	346	123	182	651	526
melicerta* x *clearei	142,662	1,085	749	310	2,144	342	124	162	628	546
boulleti* x *telchinia	290,275	738	715	307	1,760	512	113	69	694	270
All broods combined	620,496	2,889	2,570	1,101	6,560	1,200	360	413	1,973	1,342
Average across broods	206,832	963	857	367	2,187	400	120	138	658	447

[1]Markers for which SNPs were called in >=80% offspring (>10X and <200X/249X for offspring/parents respectively, GQ >=30, MQ>= 40), missing data was imputed in Beagle and Mendelian inconsistencies were excluded

[2]Markers heterozygous in mother and homozygous in father, excluding those not fitting a 1:1 ratio

[3]Markers heterozygous in father and homozygous in mother, excluding those not fitting a 1:1 ratio

[4]Markers heterozygous in both parents, excluding those not fitting 1:2:1 ratio

[6]Markers mapped to the 20 autosomes within *Joinmap* (Van Oijen and Voorrips, 2001)

Table S10. Summary of major and minor (suggestive) QTLs mapped in *H. hecale* and *H. ismenius*

Chromosome	Name[A]	Homologous colour locus[B]	Candidate gene	Phenotypic effect[C]	Cross	Scaffold(s)[D]
1	–			Variation of the FW yellow apical dots and the marginal edge of the FW band	*H. hecale melicerta x H. h. clearei*	HE672073-HE672064
7	–			Position of the proximal edge of the HW black marginal band	*H. hecale melicerta x H. h. zuleika*	HE671567
10	–			Black/orange switch near the HW costa and shape of the distal edge of the FW band	*H. hecale melicerta x H. h. clearei*	HE671252-HE668478
10	***HhAc***	***Ac* (*H. melpomene*), *Sd* (*H. erato*/*himera*), *Ac* (*H. cydno*/*pachinus*)**	***WntA***	**Size and position of black patterns close to the FW discal cell**	***H. hecale melicerta x H. h. zuleika***	**HE668478 (378)**
10	***HiAc***	***Ac* (*H. melpomene*), *Sd* (*H. erato*/*himera*), *Ac* (*H. cydno*/*pachinus*)**	***WntA*?**	**Size and position of black patterns close to the FW discal cell**	***H. ismenius boulleti x H. i. telchinia***	**HE668478 (519)**
12	–			Black/orange switch on median region of HW	*H. hecale melicerta x H. h. clearei*	HE672051
13	–			HW and proximal FW melanisation, and shape of the proximal edge of the FW band	*H. hecale melicerta x H. h. clearei*	HE670176*-HE671149
13	–			Shape of the proximal edge of the HW black marginal band and variation of the FW yellow apical dots	*H. hecale melicerta x H. h. zuleika*	HE671149-HE670666

Table S10. *Continued*

Chromosome	Name[A]	Homologous colour locus[B]	Candidate gene	Phenotypic effect[C]	Cross	Scaffold(s)[D]
15	**Fspot;** HhN	**Fspot=?;** HhN=*N*? (*H. melpomene*)		**Variation of the FW yellow apical dots (Fspot)**, shape of the distal edge of the FW band (HhN) and melanisation of the HW and proximal FW region	***H. hecale melicerta x H. h. clearei***	**HE667780 (623)**
15	–			Melanisation of the HW and the proximal FW region	*H. hecale melicerta x H. h. clearei*	HE671193
15	**Hspot; *HhN***	**Hspot=*Sb* (*H. melpomene*/*cydno*); *HhN*=*N* (*H. melpomene*)**		**Variation in the number of yellow spots on the margin of the HW (Hspot) and the presence/absence of the third row of yellow FW spots (*HhN*)**	***H. hecale melicerta x H. h. zuleika***	**HE667780 (295)**
15	*HiN*	*N* (*H. melpomene*)		Variation in the distal area of the FW band (*HiN*) and melanisation on the HW median and distal area	*H. ismenius boulleti x H. i. telchinia*	HE667780
16	–			Black/orange switch near the HW costa and shape of the distal edge of the FW band	*H. hecale melicerta x H. h. clearei*	HE668274
17	–			Shape of the distal edge of the FW band	*H. ismenius boulleti x H. i. telchinia*	HE671784-HE671089
18	**Cm**	***B, D* (*H. melpomene*), *D* (*H. erato*)**	***optix*?**	**Black/orange switch on the HW and the proximal FW region**	***H. hecale melicerta x H. h. clearei***	**HE670865 (629)**
18	***HhBr***	***Br* (*H. cydno*/*pachinus*)**	***optix*?**	**Shape of the black marginal band of the HW**	***H. hecale melicerta x H. h. zuleika***	**HE670865 (652)**
18	***HiBr***	***Br* (*H. cydno*/*pachinus*)**	***optix*?**	**Shape of the black marginal band of the HW**	***H. ismenius boulleti x H. i. telchinia***	**HE670865 (293)**

[A] Dashes correspond to unnamed QTLs. Traits segregating in Mendelian ratios are in italic script. Traits written in non-italics refer simultaneously to the quantitative trait and the QTL of major effect associated with it. Major effect loci are written in bold, minor QTLs are written in non-bold. Minor effect loci usually correspond to suggestive QTLs detected using a lower threshold (LOD>=3) and might act as modifiers of pattern elements also controlled by major loci.

[B] One of the names given to Mendelian colour loci being homologous to the QTLs in *H. hecale* and *H. ismenius* in other *Heliconius* species (shown in brackets and separated by a slash when their detection involved interspecific crosses). The equality symbol represents homology in cases where more than one pattern element is associated with the same QTL. Detailed information about the colour loci mapped in other species can be found in Table S1.

[C] Heatmaps describing the phenotypic effect of each QTL are shown in Figures 3 and S8. FW stands for forewing(s) and HW for hindwing(s).

[D] Most likely location of a given QTL on a genomic scaffold or between a pair of scaffolds (separated by a hyphen). For major effect loci, segregation patterns corresponding to those in Figure S7 are shown in brackets.

***** Unmapped scaffold.

SUPPLEMENTARY FIGURES

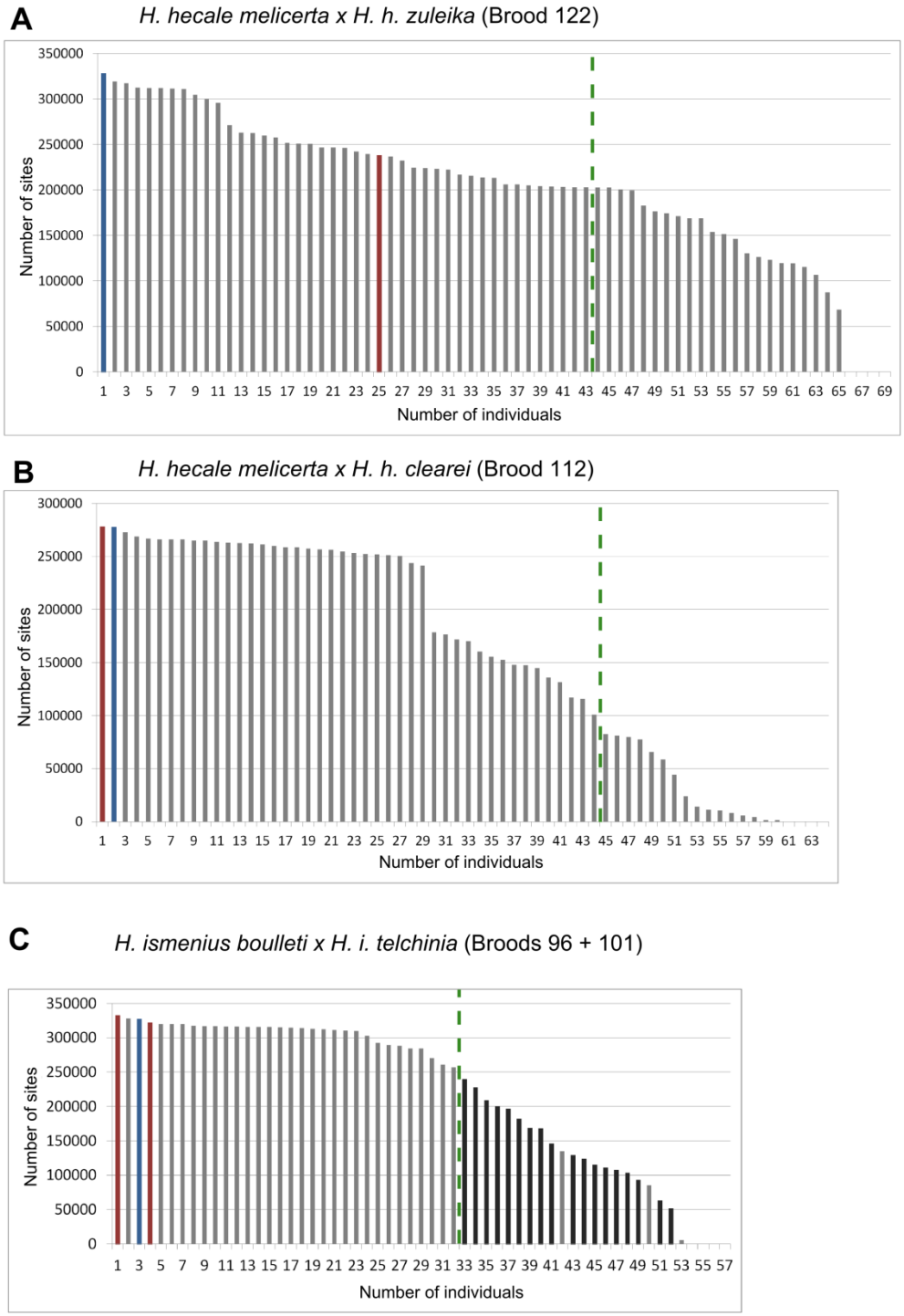

Figure S1. Number of retained positions after filtering genotype calls for coverage (>10x and <200x/249x for offspring/parents, respectively), genotype quality (GQ >=30) and mapping quality (MQ>= 40) with a custom *Perl* script (Kanchon Dasmahapatra 2012, personal communication). (**A**) *H. hecale melicerta x H. h. zuleika*, (**B**) *H. hecale melicerta* x *H. h. clearei* and (**C**) *H. ismenius boulleti* x *H. i. telchinia* broods (grey and black bars denote brood 96 and 101, respectively). In all panels, blue bars indicate the F1 father and red bars the mother(s). Only individuals left of the vertical dashed green line were retained for mapping (41, 42 and 29 offspring plus 2 backcross parents in Broods 122, 112 and 96, respectively). Due to low sequence volumes in all Brood 101 progeny, this brood was excluded from the mapping.

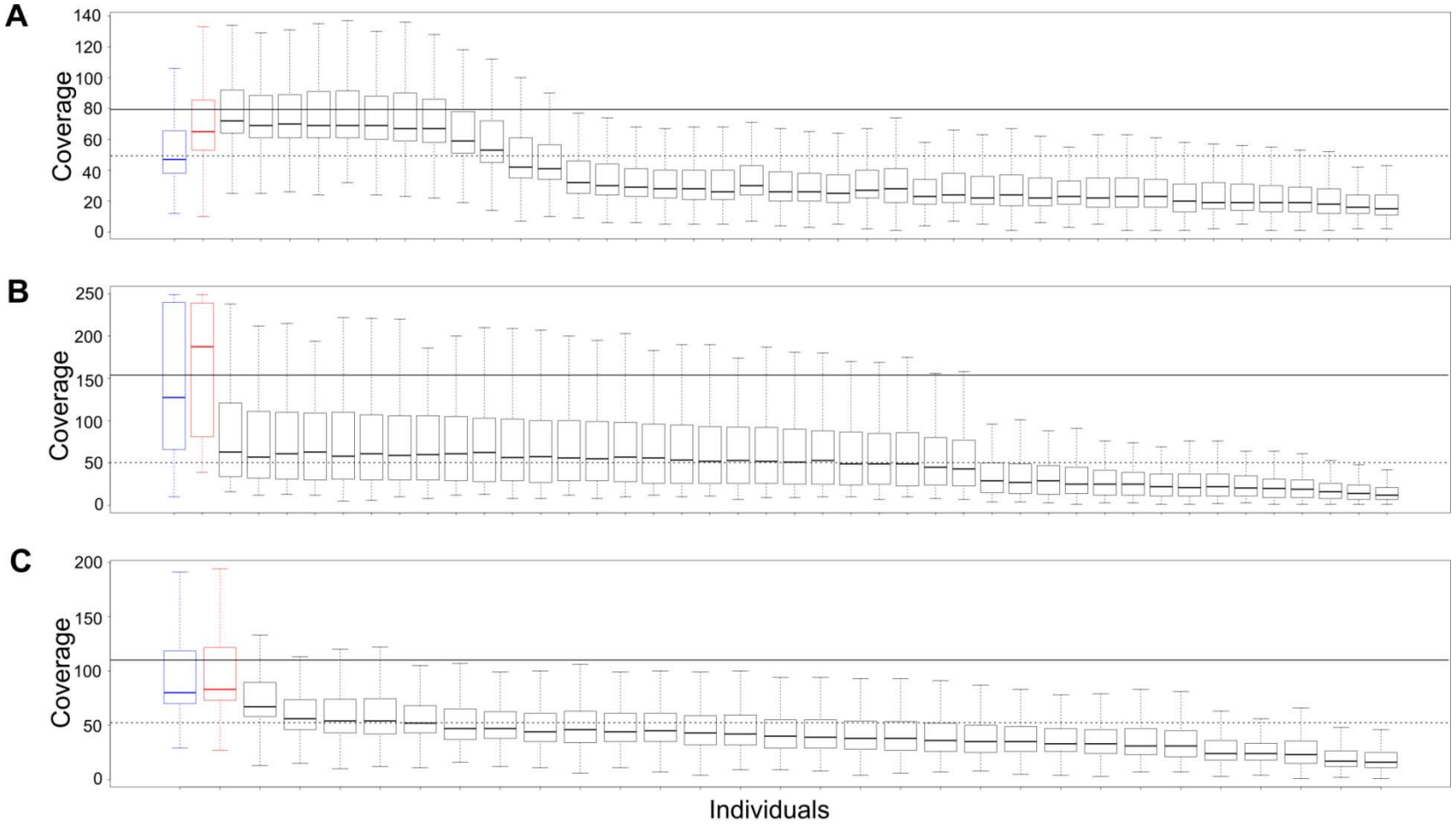

Figure S2. Distribution of sequencing depth across the set of good quality polymorphic SNPs for the chosen subsets of individuals in each type of cross. Box and whisker plots showing the median value and first and third quartiles (boxes), and the upper and lower extreme values (whiskers) for (**A**) *H. hecale melicerta* x *H. h. zuleika* (Br122), (**B**) *H. hecale melicerta* x *H. h. clearei* (Br112) and (**C**) *H. ismenius boulleti* x *H. i. telchinia* (Br96). Mean coverage for parents (solid horizontal line) and offspring (dashed horizontal line) are indicated for each family. The father (blue box) and the mother (red box) are highlighted for each cross.

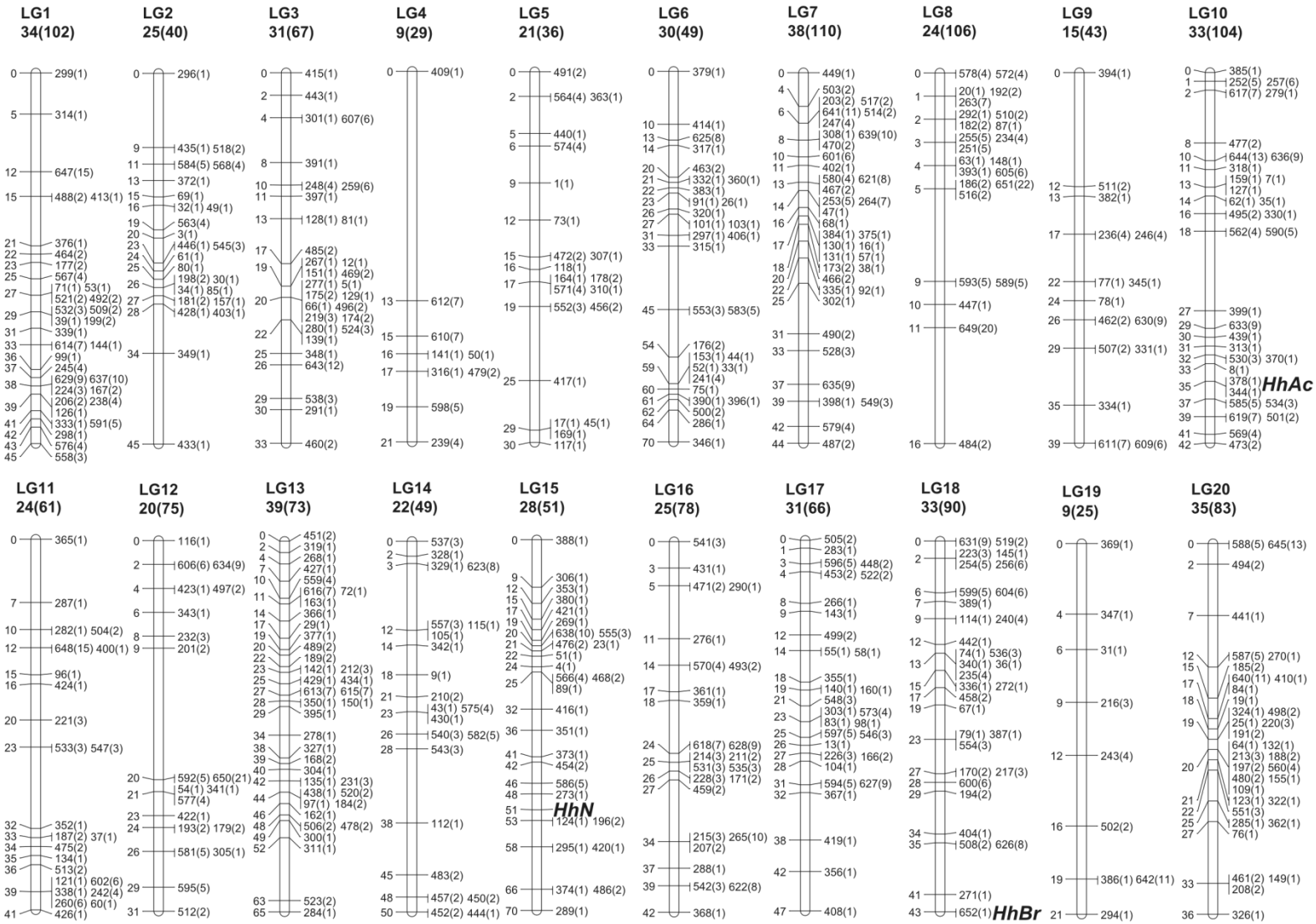

Figure S3. Linkage map of the *Heliconius hecale* genome (20 autosomes) **derived from the *H. hecale melicerta* x *H. hecale zuleika* cross**. The position of each RAD-sequencing derived marker is shown in units of recombination frequency (centimorgans). Markers were given numerical identifiers which were in turn derived from collapsing multiple supporting SNPs with identical segregation patterns (number in brackets). The total number of markers per linkage group is shown on top of each chromosome map, with the total number of SNPs in brackets. The position on the genome of wing patterning loci *HhAc, HhN* and *HhBr* is shown.

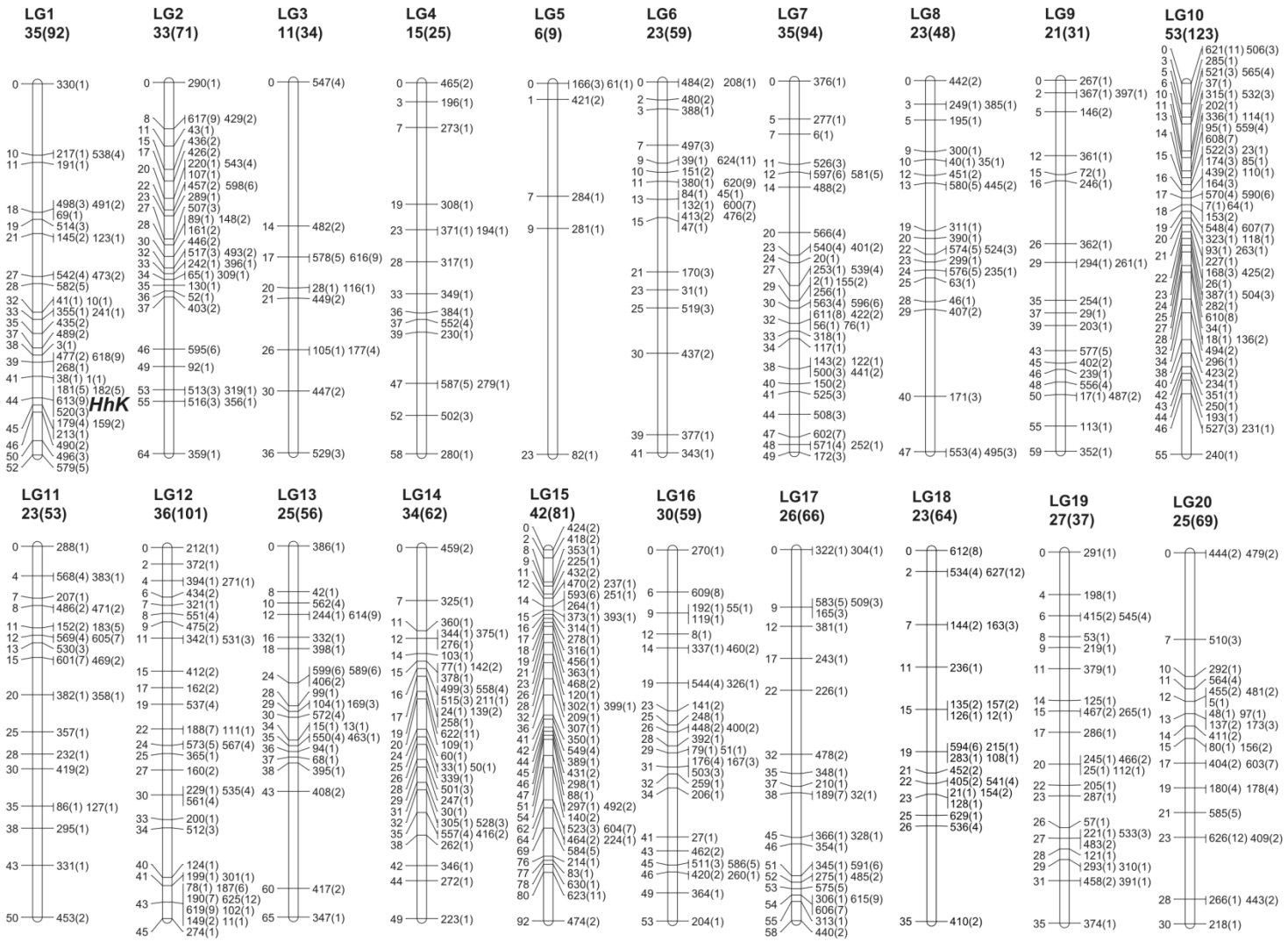

Figure S4. Linkage map of the *Heliconius hecale* genome (20 autosomes) **derived from the *H. hecale melicerta* x *H. hecale clearei* cross**. The position of each RAD-sequencing derived marker is shown in units of recombination frequency (centimorgans). Markers were given numerical identifiers which were in turn derived from collapsing multiple supporting SNPs with identical segregation patterns (number in brackets). The total number of markers per linkage group is shown on top of each chromosome map, with the total number of SNPs in brackets. The position on LG1 of the wing patterning locus *HhK* is shown.

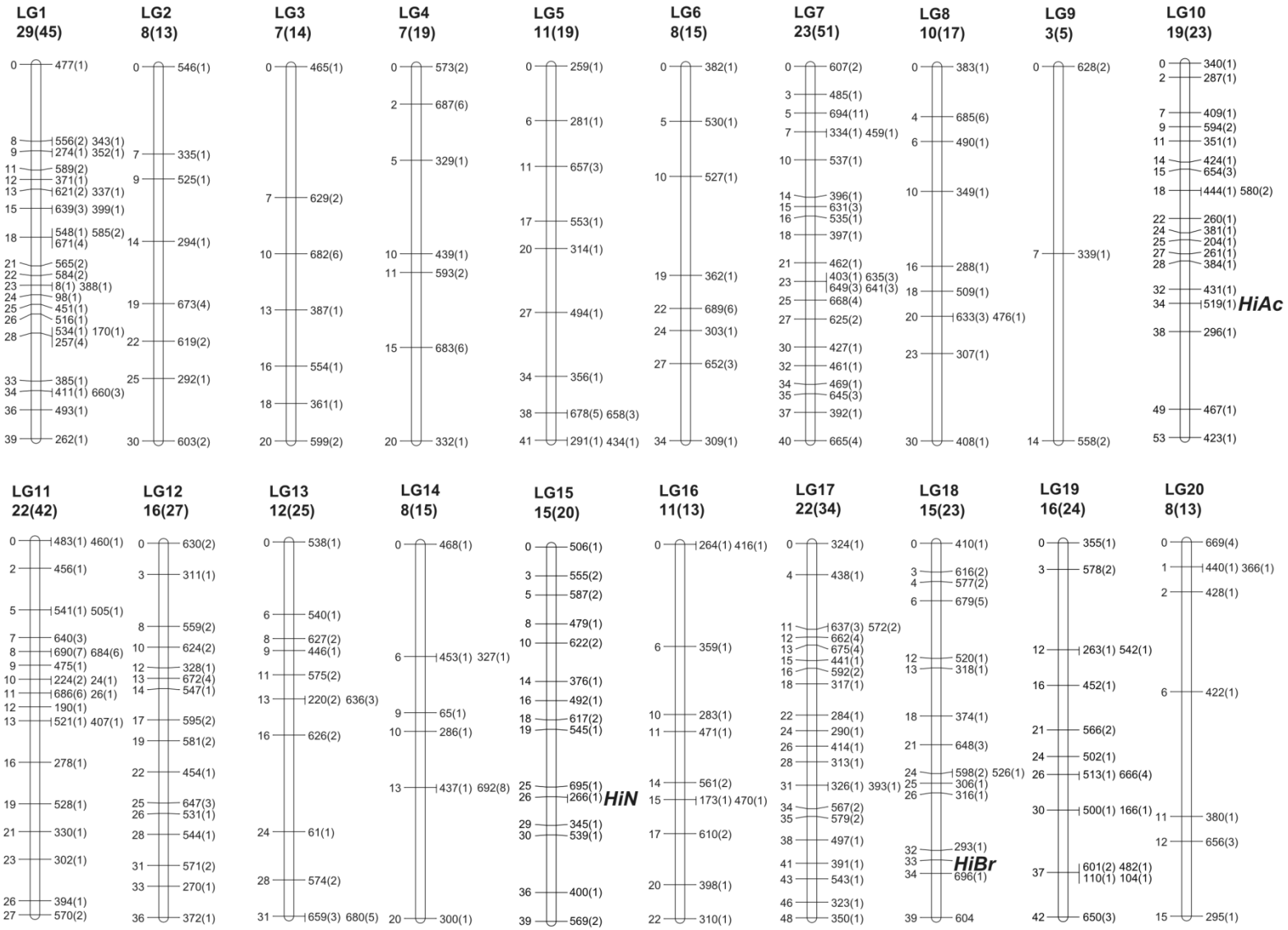

Figure S5. Linkage map of the *Heliconius ismenius* genome (20 autosomes) **derived from the *H. ismenius boulleti* x *H. ismenius telchinia* cross.** The position of each RAD-sequencing derived marker is shown in units of recombination frequency (centimorgans). Markers were given numerical identifiers which were in turn derived from collapsing multiple supporting SNPs with identical segregation patterns (number in brackets). The total number of markers per linkage group is shown on top of each chromosome map, with the total number of SNPs in brackets. The position on the genome of wing patterning loci *HiAc, HiN* and *HiBr* is shown.

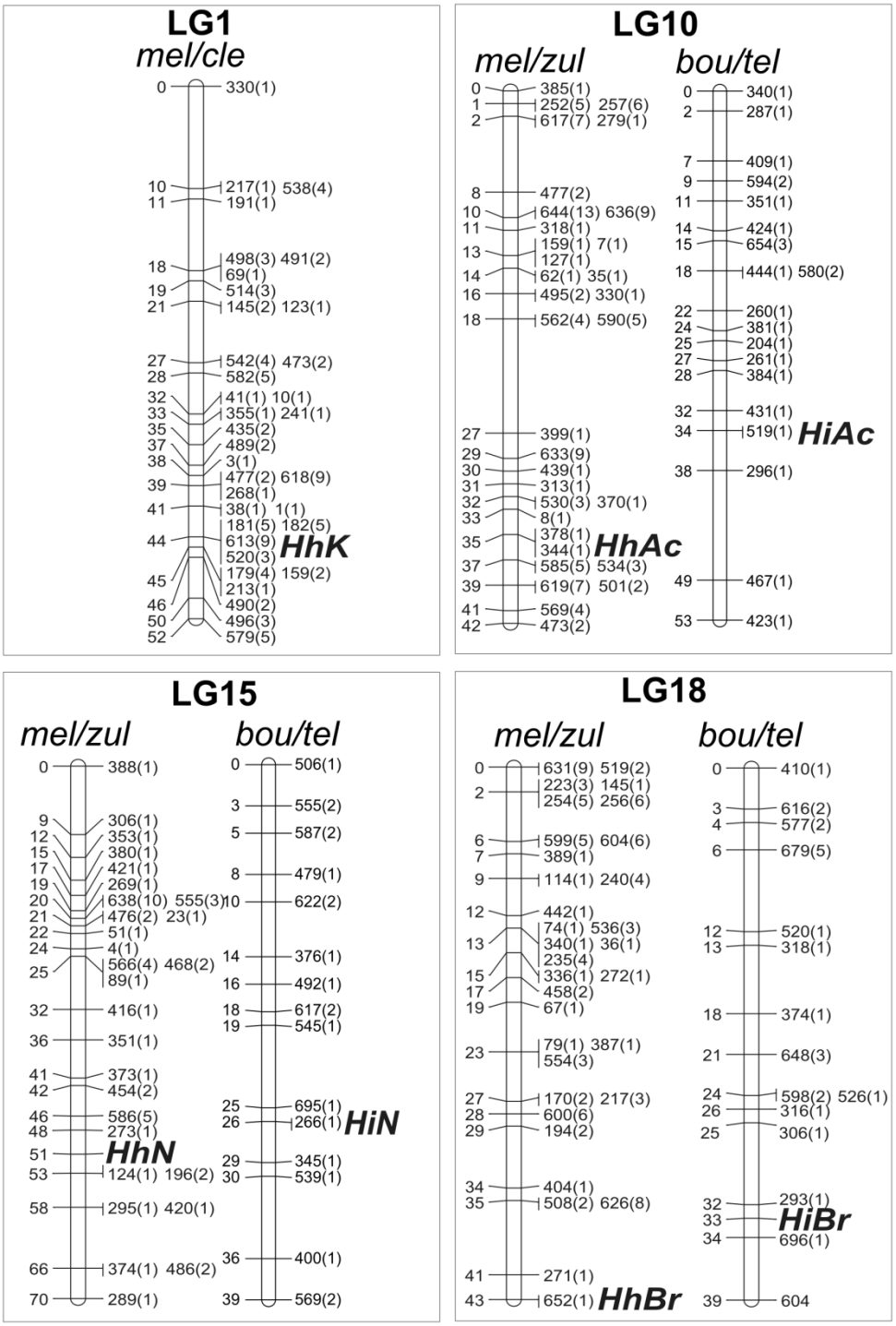

Figure S6. Genomic position (in centimorgans) for each colour locus on its linkage group (LG) in *H. hecale melicerta* x *H. h. clearei* (*mel/cle*), *H. hecale melicerta* x *H. h. zuleika* (*mel/zul*), and *H. ismenius boulleti* x *H. i. telchinia* (*bou/tel*) crosses. Markers are named by their segregation patterns (seg.pat.) collapsing multiple supporting RAD markers (number in brackets). Locus *HhK* maps to LG1, together with the genomic scaffold that contains gene *wingless* (HE671174; several SNPs collapsed to seg.pats. numbers 181 and 182), but also with markers on scaffolds HE670375 and HE671357 (seg.pats. 613+520 and 179+159+490, respectively). Loci *HhAc* and *HiAc* map to LG10. They cluster together with markers on the *WntA* scaffold scfHE668478 (seg.pat. 378+344 and 519). Loci *HhN* and *HiN* map to LG15, close to the *Yb-Sb-N/Cr/P* superscaffold (scfHE667780; seg.pat. 124+196 and 695). Loci *HhBr* and *HiBr* map to LG18. They cluster with markers on the scaffold containing the gene *optix*, scfHE670865 (seg.pat. 652 and 293+696).

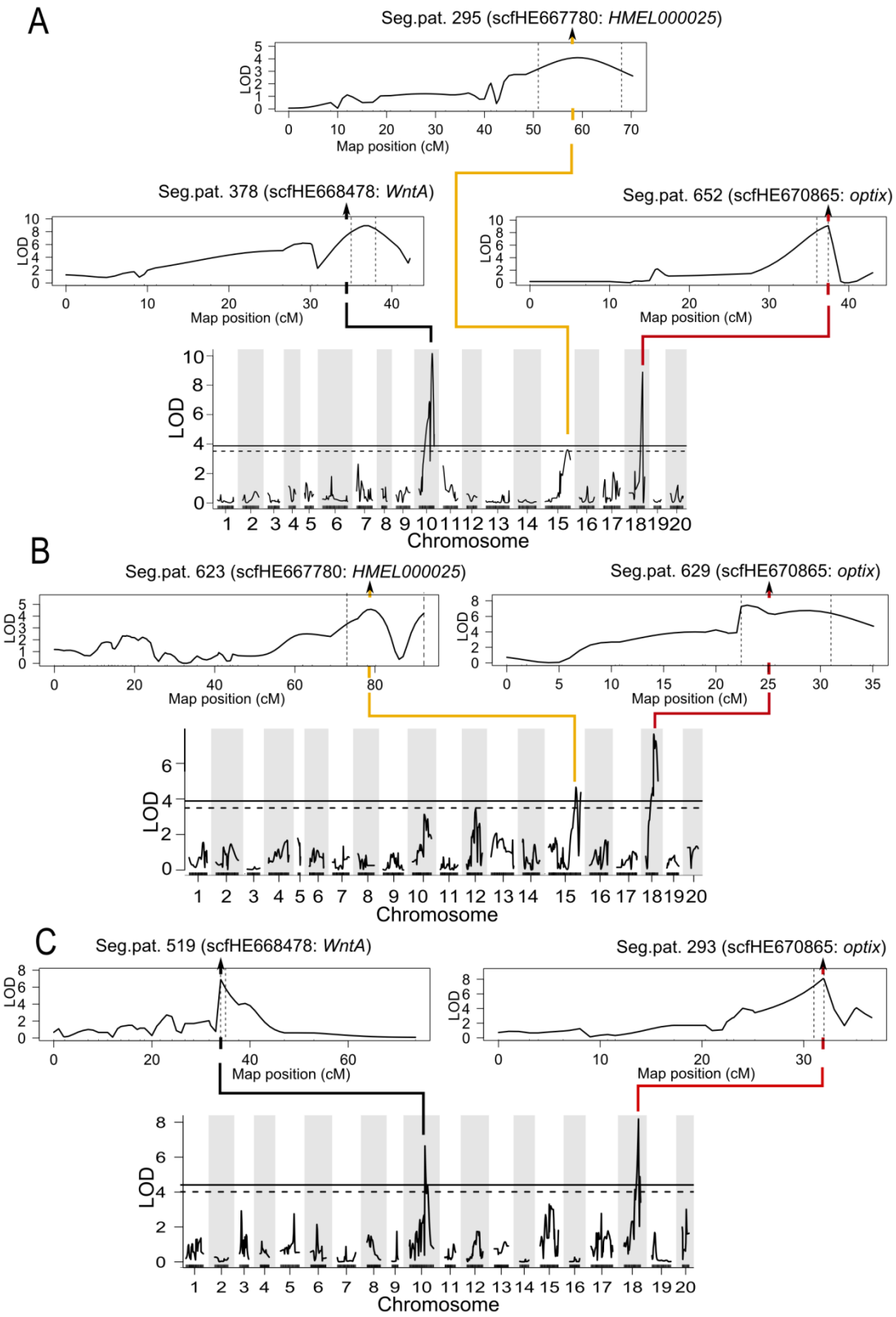

Figure S7. Detail of QTL mapping around the highest peaks of LOD score in each cross . (**A**) *H. hecale melicerta* x *H. h. zuleika*, (**B**) *H. hecale melicerta* x *H. h. clearei* and (**C**) *H. ismenius boulleti* x *H. i. telchinia*. Credible intervals around the highest peak (see also Figure 3) are delimited by vertical dashed lines. *H. melpomene* genome scaffolds (scf) containing candidate colour loci (*WntA, HMEL000025* and *optix*) are indicated for each major QTL, with the position of the corresponding RAD marker (seg.pat.) shown by arrows. Credible intervals were determined using the *bayesint* function of R/qtl with a coverage probability of 0.95.

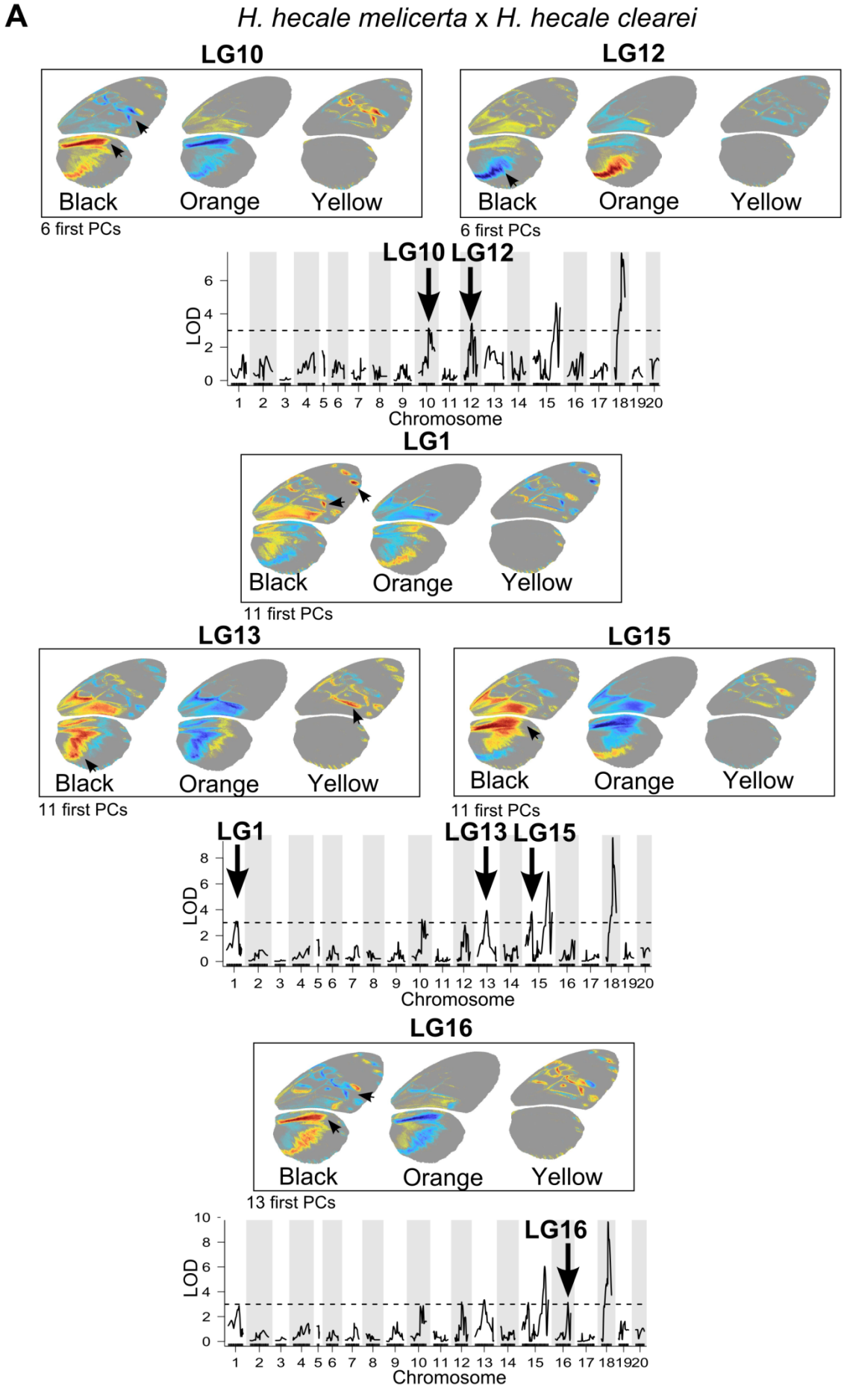
A
H. hecale melicerta x H. hecale clearei
LG10
LG12
Black
Orange
Yellow
6 first PCs
LG10 LG12
LOD
Chromosome
LG1
11 first PCs
LG13
LG15
LG1
LG13 LG15
LG16
13 first PCs

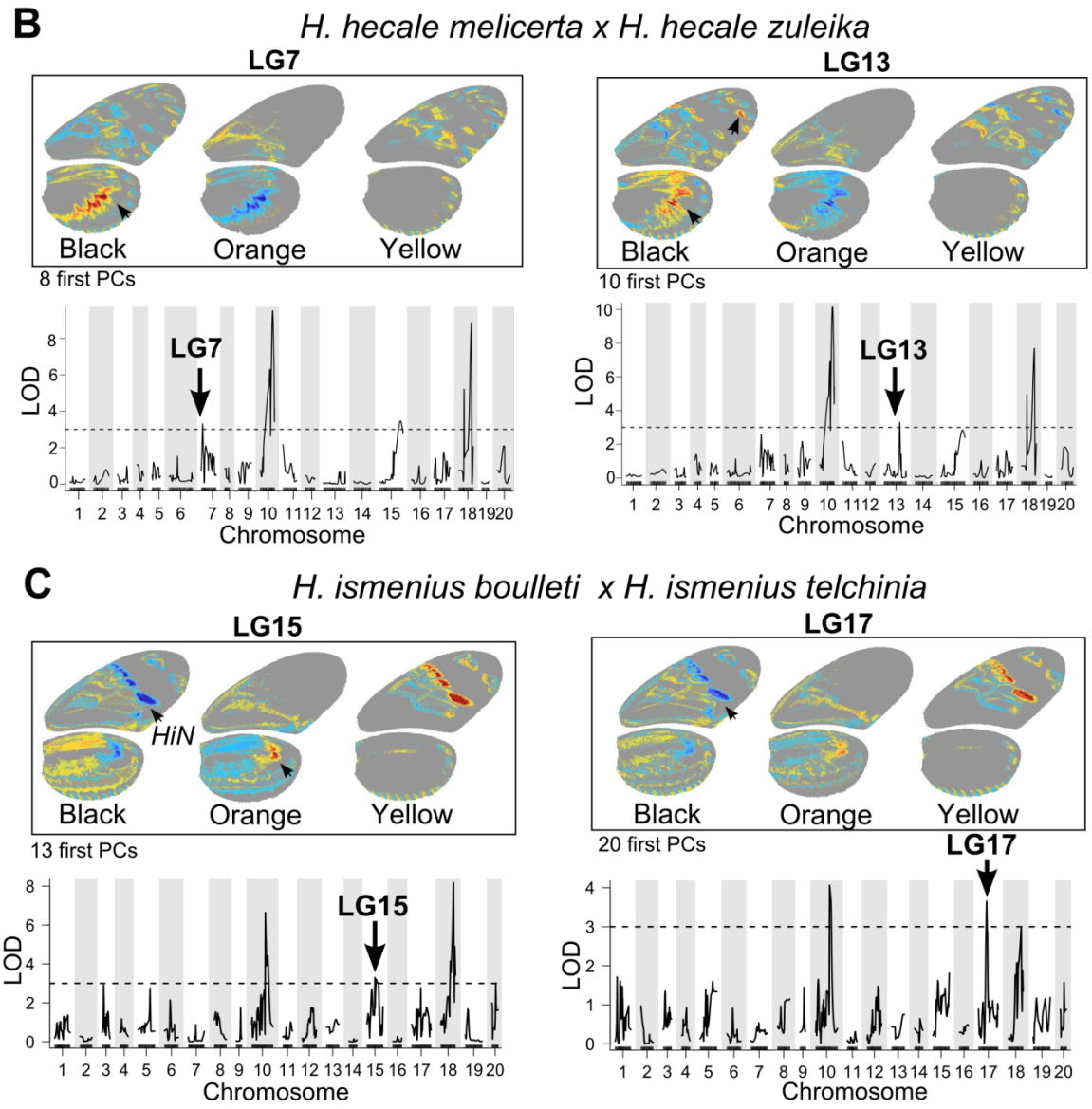

Figure S8. Genomic position and phenotypic effect of suggestive QTLs identified in the *H. hecale* and *H. ismenius* crosses. (**A**) *H. hecale melicerta* x *H. h. clearei,* (**B**) *H. hecale melicerta* x *H. h. zuleika and* (**C**) *H. ismenius boulleti* x *H. i. telchinia.* Each panel illustrates the phenotypic effect of a specific QTL (upper pane) and the genome-wide association scans (lower pane) with the targeted QTL and linkage group indicated by black arrows. The subset of principal components used in each case is stated. Coloured wing diagrams show the spatial distribution of individual QTL effects on pattern variation extracted from multivariate wing pattern analysis. Phenotypic variation is broken down into heatmaps for each of the three main colours (black, orange and yellow), representing, for every wing position, the strength of association between colour presence and allelic transition at the QTL (from blue to red). For analytical simplicity purposes, both white and yellow elements in the *H. hecale melicerta* x *H. h. clearei* cross were considered as yellow elements. Genomic plots show the genome-wide association (LOD) scan between wing pattern variation and markers on the 20 autosomes, with the conventional association threshold of LOD=3 shown with an horizontal dashed line. See Table S10 for information about the approximate genomic location of each QTL.

REFERENCES

Baxter SW, Johnston SE, Jiggins CD (2008a). Butterfly speciation and the distribution of gene effect sizes fixed during adaptation. *Heredity* **102**: 57–65.

Baxter SW, Papa R, Chamberlain N, Humphray SJ, Joron M, Morrison C, *et al.* (2008b). Convergent Evolution in the Genetic Basis of Müllerian Mimicry in *Heliconius* Butterflies. *Genetics* **180**: 1567–1577.

Broman KW, Rowe LB, Churchill GA, Paigen K (2002). Crossover interference in the mouse. *Genetics* **160**: 1123–1131.

Broman KW, Speed TP (2002). A model selection approach for the identification of quantitative trait loci in experimental crosses. *Journal of the Royal Statistical Society: Series B (Statistical Methodology)* **64**: 641–656.

Broman KW, Wu H, Sen S, Churchill GA (2003). *R/qtl:* QTL mapping in experimental crosses. *Bioinforma Oxf Engl* **19**: 889–890.

Broman KW, Sen S (2009). A Guide to QTL Mapping with *R/qtl*. Springer.

Chamberlain NL, Hill RI, Baxter SW, Jiggins CD, Kronforst MR (2011). Comparative population genetics of a mimicry locus among hybridizing *Heliconius* butterfly species. *Heredity* **107**: 200–204.

Churchill GA, Doerge RW (1994). Empirical threshold values for quantitative trait mapping. *Genetics* **138**: 963–971.

Counterman BA, Araujo-Perez F, Hines HM, Baxter SW, Morrison CM, Lindstrom DP, *et al.* (2010). Genomic Hotspots for Adaptation: The Population Genetics of Müllerian Mimicry in *Heliconius erato*. *PLoS Genet* **6**: e1000796.

Emsley MG (1964). The geographical distribution of the color-pattern components of *Heliconius erato* and *Heliconius melpomene* with genetical evidence for the systematic relationship between the two species. *Zool N Y* **49**: 245–286.

Ferguson L, Lee SF, Chamberlain N, Nadeau N, Joron M, Baxter S, *et al.* (2010). Characterization of a hotspot for mimicry: assembly of a butterfly wing transcriptome to genomic sequence at the *HmYb/Sb* locus. *Mol Ecol* **19**: 240–254.

Gallant JR, Imhoff VE, Martin A, Savage WK, Chamberlain NL, Pote BL, *et al.* (2014). Ancient homology underlies adaptive mimetic diversity across butterflies. *Nat Commun* **5**.

Gilbert LE (2003). Adaptive novelty through introgression in *Heliconius* wing patterns: evidence for shared genetic 'tool box' from synthetic hybrid zones and a theory of

diversification. In: Boggs CL, Watt WB, Ehrlich PR (eds) *Butterflies: Ecology and Evolution Taking Flight*, Univ. of Chicago Press: Chicago.

Haley CS, Knott SA (1992). A simple regression method for mapping quantitative trait loci in line crosses using flanking markers. *Heredity* **69**: 315–324.

Jiggins CD, McMillan WO (1997). The genetic basis of an adaptive radiation: warning colour in two *Heliconius* species. *Proc R Soc B Biol Sci* **264**: 1167–1175.

Jiggins CD, Mavarez J, Beltrán M, McMillan WO, Johnston JS, Bermingham E (2005). A Genetic Linkage Map of the Mimetic Butterfly *Heliconius melpomene*. *Genetics* **171**: 557–570.

Jones RT, Salazar PA, ffrench-Constant RH, Jiggins CD, Joron M (2011). Evolution of a mimicry supergene from a multilocus architecture. *Proc Biol Sci* **279**: 316–325.

Joron M, Papa R, Beltrán M, Chamberlain N, Mavárez J, Baxter S, *et al.* (2006). A Conserved Supergene Locus Controls Colour Pattern Diversity in *Heliconius* Butterflies. *PLoS Biol* **4**: e303.

Kapan DD (1998). Divergent natural selection and müllerian mimicry in polymorphic *Heliconius cydno* (Lepidoptera: Nymphalidae). Doctoral dissertation, University of British Columbia.

Kapan DD, Flanagan NS, Tobler A, Papa R, Reed RD, Gonzalez JA, *et al.* (2006). Localization of Müllerian Mimicry Genes on a Dense Linkage Map of *Heliconius erato*. *Genetics* **173**: 735–757.

Knott SA, Haley CS (2000). Multitrait least squares for quantitative trait loci detection. *Genetics* **156**: 899–911.

Kronforst MR, Kapan DD, Gilbert LE (2006a). Parallel Genetic Architecture of Parallel Adaptive Radiations in Mimetic *Heliconius* Butterflies. *Genetics* **174**: 535–539.

Kronforst MR, Young LG, Kapan DD, McNeely C, O'Neill RJ, Gilbert LE (2006b). Linkage of butterfly mate preference and wing color preference cue at the genomic location of *wingless*. *Proc Natl Acad Sci* **103**: 6575–6580.

Leamy LJ, Klingenberg CP, Sherratt E, Wolf JB, Cheverud JM (2008). A search for quantitative trait loci exhibiting imprinting effects on mouse mandible size and shape. *Heredity* **101**: 518–526.

Linares M (1996). The Genetics of the Mimetic Coloration in the Butterfly *Heliconius cydno weymeri*. *J Hered* **87**: 142–149.

Linares M (1997). Origin of neotropical mimetic biodiversity from a threeway hybrid zone of *Heliconius cydno* butterflies. In: *H. Ulrich*, Proceedings of the International Symposium on Biodiversity and Systematics in Tropical Ecosystems. Zoologisches Forschungsinstitut und Museum Alexander Koenig: Bonn, pp 93–108.

Mallet J (1989). The Genetics of Warning Colour in Peruvian Hybrid Zones of *Heliconius erato* and *H. melpomene*. *Proc R Soc Lond B Biol Sci* **236**: 163–185.

Manichaikul A, Dupuis J, Sen S, Broman KW (2006). Poor performance of bootstrap confidence intervals for the location of a quantitative trait locus. *Genetics* **174**: 481–489.

Manichaikul A, Moon JY, Sen S, Yandell BS, Broman KW (2009). A model selection approach for the identification of quantitative trait loci in experimental crosses, allowing epistasis. *Genetics* **181**: 1077–1086.

Martin A, Papa R, Nadeau NJ, Hill RI, Counterman BA, Halder G, *et al.* (2012). Diversification of complex butterfly wing patterns by repeated regulatory evolution of a *Wnt* ligand. *Proc Natl Acad Sci U S A* **109**: 12632–12637.

Martin A, McCulloch KJ, Patel NH, Briscoe AD, Gilbert LE, Reed RD (2014). Multiple recent co-options of *Optix* associated with novel traits in adaptive butterfly wing radiations. *EvoDevo* **5**: 7.

Nadeau N, Ruiz M, Salazar P, Counterman B, Medina JA, Ortiz-Zuazaga H, *et al.* (2014). Population genomics of parallel hybrid zones in the mimetic butterflies, *H. melpomene* and *H. erato*. *Genome Res*: gr.169292.113.

Naisbit RE, Jiggins CD, Mallet J (2003). Mimicry: developmental genes that contribute to speciation. *Evol Dev* **5**: 269–280.

Nijhout HF, Wray GA, Gilbert LE (1990). An analysis of the phenotypic effects of certain colour pattern genes in *Heliconius* (Lepidoptera: Nymphalidae). *Biol J Linn Soc* **40**: 357–372.

Papa R, Martin A, Reed RD (2008). Genomic hotspots of adaptation in butterfly wing pattern evolution. *Curr Opin Genet Dev* **18**: 559–564.

Papa R, Kapan DD, Counterman BA, Maldonado K, Lindstrom DP, Reed RD, *et al.* (2013). Multi-Allelic Major Effect Genes Interact with Minor Effect QTLs to Control Adaptive Color Pattern Variation in *Heliconius erato*. *PLoS ONE* **8**: e57033.

Pillai KCS (1967). Upper percentage points of the largest root of a matrix in multivariate analysis. *Biometrika* **54**: 189.

Reed RD, Papa R, Martin A, Hines HM, Counterman BA, Pardo-Diaz C, *et al.* (2011). *optix* drives the repeated convergent evolution of butterfly wing pattern mimicry. *Science* **333**: 1137–1141.

Sheppard PM, Turner JRG, Brown KS, Benson WW, Singer MC (1985). Genetics and the Evolution of Muellerian Mimicry in *Heliconius* Butterflies. *Philos Trans R Soc Lond B Biol Sci* **308**: 433–610.

Tobler A, Kapan D, Flanagan NS, Gonzalez C, Peterson E, Jiggins CD, *et al.* (2004). First-generation linkage map of the warningly colored butterfly *Heliconius erato*. *Heredity* **94**: 408–417.

Turner JRG, Crane J (1962). The genetics of some polymorphic forms of the butterflies *Heliconius melpomene* Linnaeus and *Heliconius erato* Linnaeus. I. Major genes. *Zool N Y* **47**: 141–152.

Turner JRG (1972). The genetics of some polymorphic forms of the butterflies *Heliconius melpomene* (Linnaeus) and *Heliconius erato* (Linnaeus). II. The hybridization of subspecies of *H. melpomene* from Surinam and Trinidad. *Zoologica* **56**: 125–157.

Van Oijen JW, Voorrips RE (2001). Joinmap Version 3.0, software for the calculation of genetic linkage maps. *Plant Res Int Wagening Neth*.